



# Rockfall Hazard Assessment Around Ankara Citadel (Turkey) Using Rockfall Analyses and Hazard Rating System

Nyein Ei San · Tamer Topal · Muge K. Akin

Received: 9 November 2019 / Accepted: 28 February 2020 / Published online: 9 March 2020  
© Springer Nature Switzerland AG 2020

**Abstract** Ankara Citadel which is one of the important cultural heritages in Turkey settles in the oldest part of Ankara. Rockfall event has occurred around the Citadel located on a steep hill where andesite is exposed. The rockfall problem causes a great risk to the surrounding area where road, school, floral shops, car parking. Therefore, the major aim of this research is to reveal the rockfall risk around the castle. The rockfall problems around the Ankara Citadel may be linked with weathering, freezing–thawing, earthquake, and cooling joints, and effects or combination of these in the rock units. The rockfall-related hazard at the Citadel is assessed by 2-D rockfall analyses along several profiles in this investigation. Field observations and stability analyses (kinematic and limit equilibrium) of the slopes reveal that there exist many blocks ready to fall down. Four different andesite block sizes measured in the field are separately analyzed on the basis of bounce height, fall-

out distance, velocity and kinetic energy of the blocks. The obtained data are evaluated to define the possible rockfall-based hazard zones. Based on the danger zones acquired from the rockfall analyses, the removal of the fallen and loosen andesite blocks and the installation of catch barriers with suggested properties are recommended. Besides, the risk integrated into rockfall hazard rating system on the basis of structural and morphological criteria of the rock mass reveals that medium risk category to be mitigated by light remedial measures for the indicative protection exists in the study area.

**Keywords** Andesite · Ankara citadel · Rockfall analysis · Zonation map · Turkey · Rockfall hazard rating system

## 1 Introduction

Rockfall is an event where rock is separated from the main geological material by falling, sliding, or toppling that falls down along a cliff. The rock moves down in the form of free fall, bouncing and rolling and sliding (Varnes 1978; Wang and Lee 2010). The rockfall event may be controlled by discontinuities (fracture, joint, bedding, schistosity, etc.), weathering, freezing–thawing, precipitation, earthquake, wave attack, tree roots, man-made activity or the combination of all these factors (Chen et al. 1994; Wasowski

---

N. E. San  
Geological Engineer, MSc., Thida Street, No:73(A),  
Tamwe Township, Yangon 11181, Myanmar

T. Topal  
Department of Geological Engineering, METU,  
06800 Ankara, Turkey

M. K. Akin (✉)  
Department of Civil Engineering, Faculty of Engineering,  
AGU, 38080 Kayseri, Turkey  
e-mail: mugeakink@gmail.com; muge.akin@agu.edu.tr

and Gaudio 2000; Marzorati et al. 2002; Dorren 2003; Topal et al. 2007, 2012; Krautblatter and Moser 2009; Tunusluoglu and Zorlu 2009; Binal and Ercanoglu 2010; Wick et al. 2010; Kaya and Topal 2015; Mineo et al. 2018). Urban areas, engineering structures and human beings are adversely affected by the rockfall events (Chau et al. 1998, 2003; Choi et al. 2009; Antoniou and Lekkas 2010; Chiessi et al. 2010; Pellicani et al. 2016). Therefore, rockfall analyses are performed with characteristic parameters (Ansari et al. 2018; Asteriou and Tsiambaos 2018; Zhu et al. 2018) and remedial measures are considered in rockfall-prone areas (Ritchie 1963; Paronuzzi 1989; Peila et al. 1998; Nicot et al. 2001; Raetzo et al. 2002; Crosta and Agliardi 2003; Corominas et al. 2005; Jaboyedoff et al. 2005; Topal et al. 2006; Fell et al. 2008; Straub and Schubert 2008; Agliardi et al. 2009; Peila and Ronco 2009; Topal et al. 2012; Dinçer et al. 2016; Gül et al. 2016; Basharat et al. 2012, 2014; Basharat and Yasir 2018; Chun et al. 2018; Korkanç et al. 2018).

For the rockfall analysis, various techniques are available such as experimental, empirical, and modeling can be considered (Giani 1992; Evans and Hungr 1993; Okura et al. 2000; Copons et al. 2009; Masuya et al. 2009; Tunusluoglu and Zorlu 2009; Binal and Ercanoglu 2010; Rammer et al. 2010; de Almeida and Kullberg 2011; Jaboyedoff et al. 2012). Modeling may be implemented using by means of two-dimensional (2-D) and/or three dimensional (3-D) softwares in order to envisage block trajectory paths, bounce height, kinetic energy, run-out distance and velocity of the rocks (Bozzolo et al. 1988; Hungr and Evans 1988; Spang and Rautenstrauch 1988; Scioldo 1991; Azzoni et al. 1995; Guzzetti et al. 2002, 2003; Agliardi and Crosta 2003; Schweigl et al. 2003; Dorren et al. 2004, 2006; Crosta and Agliardi 2004; Perret et al. 2004; Jaboyedoff et al. 2005; Wiczorek et al. 2008; Bigot et al. 2009; Bourrier et al. 2009; Budetta 2010; Jaboyedoff and Labiouse 2011; Katz et al. 2011; Mazzoccola and Sciesa 2000; Mineo et al. 2018; Rouiller & Macro 1997; Fanos and Pradhan 2019). Although 2-D models use rockfall physics and provide probability information, the models cannot include the dynamic and geometric effect of 3-D topography (Basharat and Yasir 2018). Most of the pitfalls of 2-D rockfall modelling have been overcome by 3-D modelling (Jaboyedoff et al. 2005; Chen et al. 2013). However, few of the 3-D softwares for rockfall run-out distance are easily handy (Crosta and Agliardi 2004;

RocPro3D 2014). Therefore, prediction of the run-out distance is still a difficult job in engineering practice (Basharat and Yasir 2018).

Full 3-D slope surfaces mostly preferred in 3-D models to model the rockfall phenomenon properly. Some of the softwares such as STONE (Guzzetti et al. 2002), HY-STONE (Crosta and Agliardi 2004), Rockyfor3-D (Dorren et al. 2004), RAMMS: Rockfall (Christen et al. 2007), and RocPro3D (RocPro3D 2014) are made use of to perform the rockfall analyses considering the rock fragment shape and topography (Chen et al. 2013).

Depending on the different type of slope stability analyses, some of the rockfall incidents require both kinematic analyses and classification systems of failure mechanism types. For these types of the failure classifications, mostly rockfall hazard rating systems are preferred especially for the highway rockfall problems (Youssef et al. 2003; Maerz et al. 2015). Several qualitative rockfall hazard rating systems (RHRSs) have been developed which are used by different authorities for the worldwide. Some of the rating systems are summarized below (Aqeel 2018).

The Oregon Department of Transportation introduced a Rockfall Hazard Rating System to provide information about the man made steep area susceptible to hazardous rockfall closer to the roads. It not only gives the most hazardous cases but also lends to monitor and maintain the road for the essential precautions. Oregon-RHRS (Pierson and Van-Vickle 1993), Rockfall Hazard Rating System for Ontario, Canada (RHRON) (Franklin and Senior 1997), New Priority Classification Systems (NPCSS) for Hong Kong, China (Wong 1998), Highway Slope Instability Management System (HiSIMS) for Tennessee (Miller 2003), Missouri Rockfall Hazard Rating System (MORFH-RS, Maerz et al. 2004, 2005), Modified Rockfall Hazard Rating System of Italy (mRHRS-Italy) (Budetta 2004), Rock Cut Stability Assessment (RCSA) of Spain (Uribe-Etxebarria et al. 2005), Rockfall Hazard Rating Matrix (RHRM) for Ohio (Woodard and Shakoor 2005), Utah Department of Transportation-Rockfall Hazard Rating System (DOTRHRS) (Pack et al. 2006), New York DOT Rock Slope Rating Procedure (New York Department of Transportation (NYDOT) 2007), Colorado Rockfall Hazard Rating System (CRHRS) (Russell et al. 2008), and modified Colorado-RHRS (Santi et al. 2009), Rockfall Hazard Rating System of Saudi Arabia

(RHRS-SA) (Maerz et al. 2015), Evolving Rockfall Hazard Assessment (ERHA) of Australia are some of the rockfall hazard assessment methods (Ferrari et al. 2017).

Rockfall is an important disaster that may happen in Turkey. Reported events from 1950 to 2008 indicate that a total of 2956 rockfalls occurred in 79 provinces affecting 1703 settlements and 22,157 victims (Gökce et al. 2008). The capital city Ankara is one of these provinces adversely affected by rockfall, whereas Altındag district is the most affected area in the city. Ankara Citadel (Castle) is a famous historical structure (Fig. 1). The whole Citadel consists of inner and outer circles (Fig. 2). The inner circle situated at the top of the hill is mainly from Byzantine era with some preserved the historical heritages in this section. This inner circle (wall) also called the castle is the oldest part of the whole structure. It has a length of 350 m along north–south direction and a width of nearly 180 m on east–west direction. On the other hand, the outer circle built around the west and south parts of the castle are 100–150 m away from each other. A group of structures was built downwards for the protection of the valley (Tokmak 2005). The northern part of the Ankara Citadel is characterized by a steep topography with a maximum slope height of 135 m. There are road, school, floral shops, and car parking in the northern section of the hill. There exist several fallen rocks stopped very close to the road (Fig. 3). Ankara has a climate with snowy and cold winters, and dry and hot summers. Correspondingly, freezing–thawing processes are effective in winter, besides rainfall mostly occur during the spring and autumn in that region.



**Fig. 1** Ankara Citadel and its surrounding

This study aims to assess rockfall hazard nearby the Ankara Citadel and recommend proper remedial measures on the basis of the results of the analyses, and evaluate risk based on rockfall hazard rating system. The study was mainly performed on the eastern and northern parts of the hill where steep slopes and fallen rocks exist. Scanline survey at 21 different locations, sampling, laboratory studies were performed to acquire data for the slope stability and rockfall analyses as part of this study. Potential rockfall sources were firstly defined in the field. The fallen block sizes were calculated to provide data for the rockfall analyses. L-type hammer was used for the Schmidt rebound measurements. Kinematic and limit equilibrium analyses along the slopes were implemented for the study area. Then, two dimensional rockfall analyses of the study area were completed along the profiles to assess danger zone around the Citadel. For different block sizes and weights, the analyses were executed to assess bounce height, fall-out distance with block trajectory, kinetic energy and velocity of the blocks. Depending on the obtained danger zone and field inspections, the most suitable risk mitigation methodologies were suggested for the area. Then, rockfall hazard of the area was evaluated using a rating method suitable for historical sites.

## 2 Geological Setting of the Study Area

Upper Miocene Mamak formation is the main lithological unit observed in the study area (Akyürek et al. 1997) (Fig. 4). Although it contains agglomerate, tuff, andesite and basalt, andesite having steeply joints is the dominant rock type exposed in the study area. The andesite is formed during Miocene (Erol 1961; Erentöz 1975). The rock is mostly pinkish grey and slightly to moderately weathered. The highly fractured andesite has cooling joints and flow layers forming the steep topographic features at different elevations around the Ankara Citadel (San 2017). The petrographic analysis of the andesite mainly points out the presence of plagioclase, hornblende and biotite. According to Tokmak (2005), some volcanogenic fragments, opaque amorphous formations and clay minerals can be seen as secondary minerals in the andesite.

**Fig. 2** Location map of the study area with plan of the Ankara Citadel

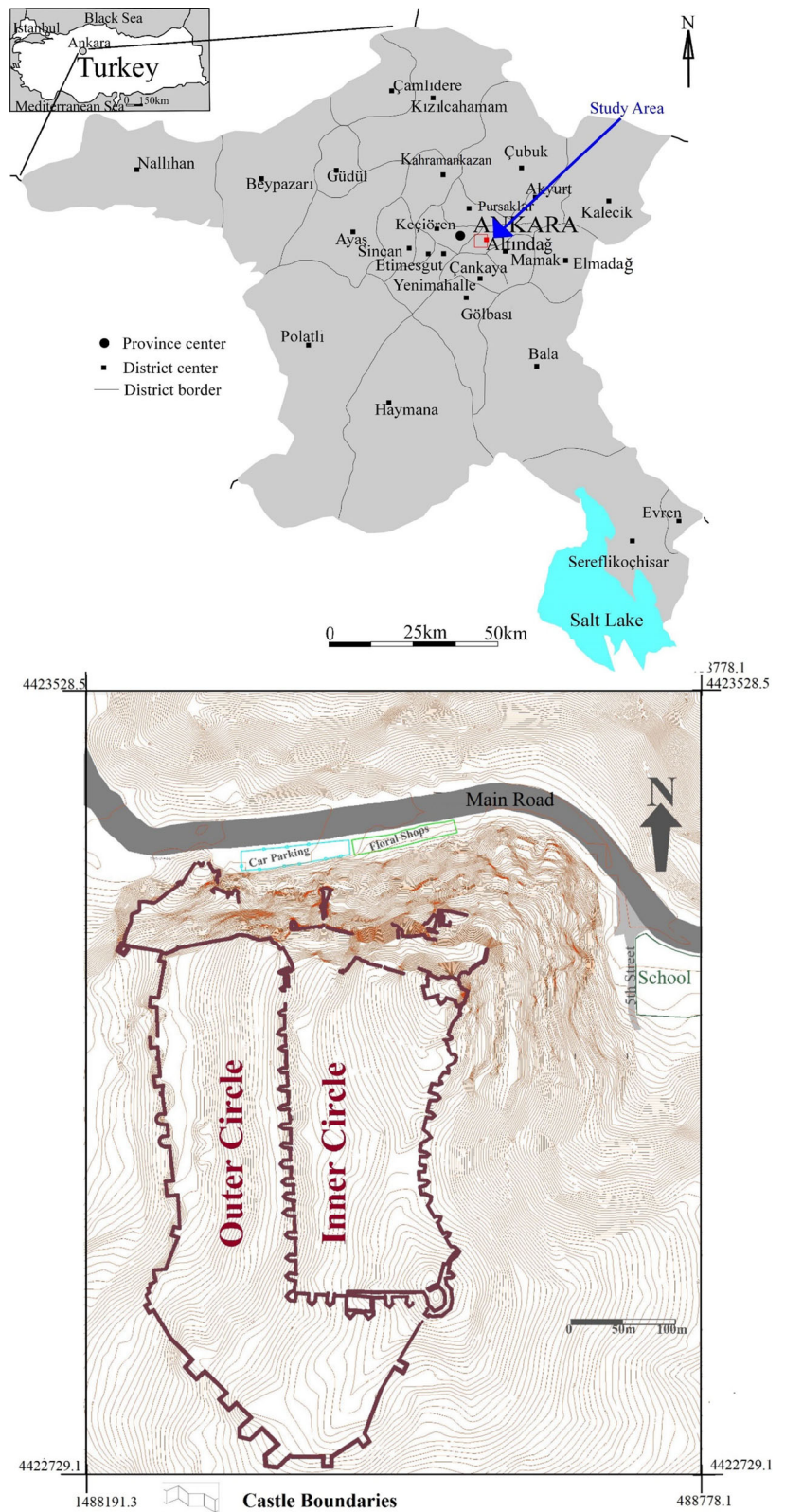




**Fig. 3** Fallen blocks seen near the floral shops and the road

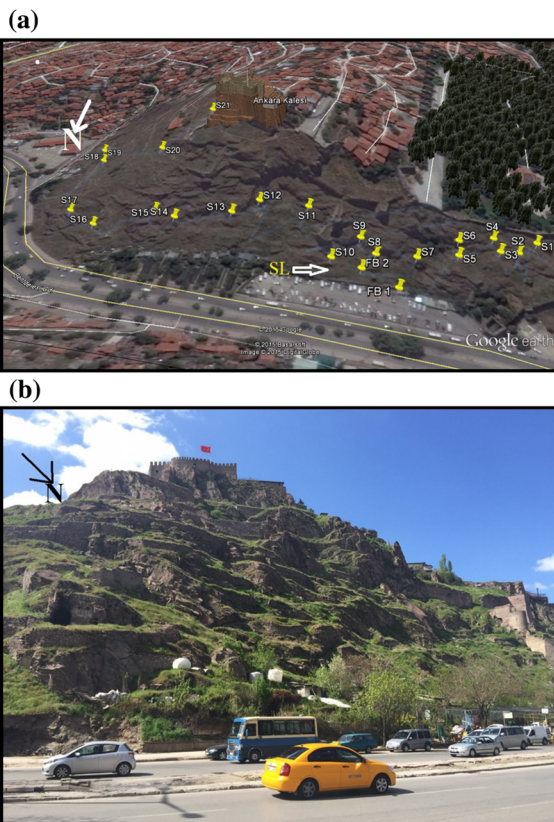


**Fig. 4** **a** Scanline survey (S) and fallen block (FB) locations, **b** Photograph of the northern part of the Ankara Citadel where measurements were done

No active faults exist in the close vicinity of the Ankara Citadel. The study area is situated within the third degree earthquake zone in Turkey ( $0.3 g >$

$PGA > 0.2 g$ ) (AFAD 1996). According to the new building earthquake code the site-specific PGA (peak ground acceleration) values should be evaluated for different site conditions (TBC 2018). The Citadel is approximately 105 km away from the North Anatolian Fault Zone (NAFZ) which is seismically active and may trigger the rockfall events.

### 3 Field and Laboratory Investigations

The area was studied to detect rockfall source areas, assess the properties of the fallen rocks, and explore the discontinuity properties of the andesite. Field data were obtained at 21 stops with scanline surveys where clear outcrops are seen and 2 fallen block spots. Coordinates of every stop were recorded with GPS and marked on Google Earth view (Fig. 4).

At each stop, discontinuity measurements through scan line surveys were carried out according to ISRM (1981, 2007) and Priest (1993). As part of the survey, orientation, spacing, aperture, infilling, persistence, wall strength, roughness, weathering, and groundwater condition of the discontinuities were measured (San 2017).

The field studies reveal that there exist some blocks already fallen in the past. The data (1941 discontinuity measurements in total) of the scanline survey at each stop and altogether around the castle were contoured (Fig. 5) using Dips 6.0 software (Rocscience 2015a). There are flow layers of the andesite with nearly low dip amount in the area. They can be traced easily and mainly scattered around the center of the contour diagram as can be seen in Fig. 5. Several steeply dipping cooling joints developed in different directions almost perpendicular to the flow layers also exist in the area. This indicates that the andesite is highly-jointed (Fig. 6). The joints have persistence dominantly  $< 5$  m. However, it may locally reach around 15 m. The spacing of the discontinuities ranges between 2 and 200 cm (moderately narrow to very wide) with a concentration mostly around 20–60 cm (wide). The apertures are generally tight with clay filling (maximum 2 cm) near the surface. Nevertheless, no infill material exist along the flow layers due to their low dip angles. The other properties of the flow layers are observed to be similar to the cooling joints. The Schmidt hardness rebound values range between 25 and 41. The mass weathering of the andesite is in

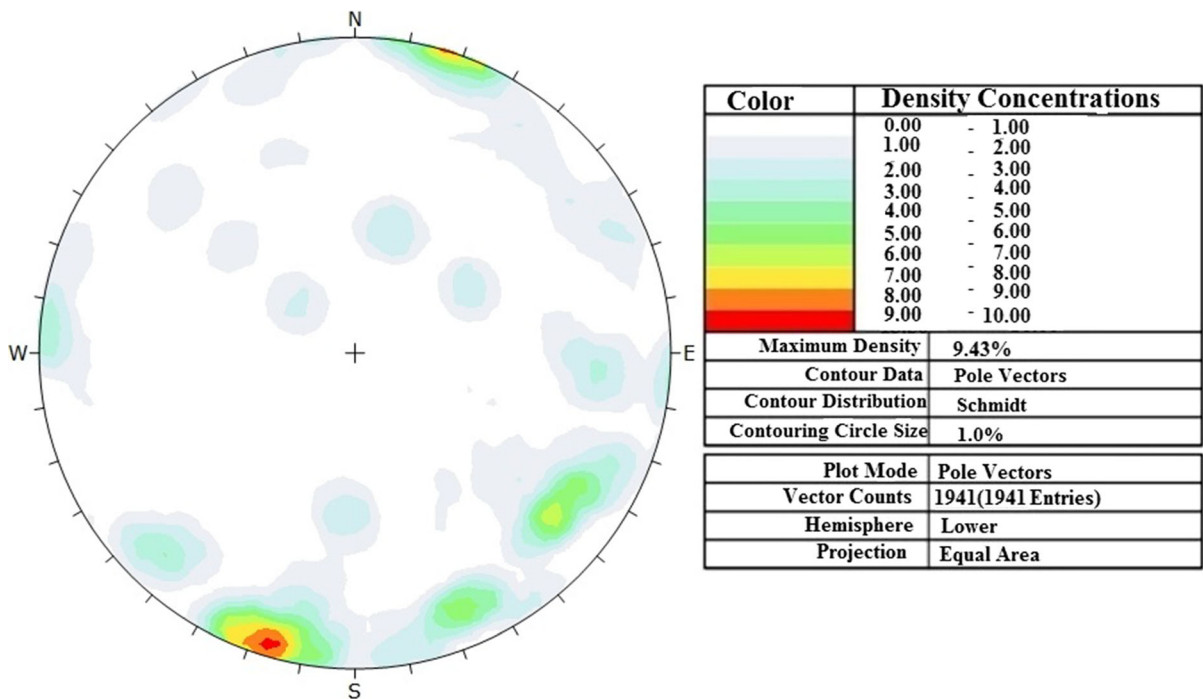


**Fig. 5** Contour diagram of the discontinuities measured during the scanline survey



**Fig. 6** Highly-jointed andesite at 4th (S4) location

slightly to moderately weathered category. Undulating rough discontinuity surfaces of the rock is observed in the field. Schmidt rebound hammer results converted to the strength values using the method suggested by Deere and Miller (1966) indicate that joint wall compressive strength (JCS) is about 3.55 MPa. The groundwater is not observed in the study area. Besides, the rockfall sources areas were located visually in the field to achieve rockfall analyses on the eastern and northern sides of the Ankara Citadel. Map showing the rockfall source areas is presented in Fig. 7. The

biggest fallen block has a dimension of  $160 \times 80 \times 60$  cm corresponding to a weight of nearly 1800 kg. Although there is a possibility that some larger blocks felt but fractured during bouncing, the authors have rarely observed clear evidences of such conditions during the field studies. Additionally, the biggest fallen block size is in well agreement with the measured spacing ranges of the discontinuities. Therefore, the biggest fallen block weight was considered as the worst case in the rockfall analyses. Several blocks were also obtained from the field taken to determine identify the engineering properties of the rock. Oriented NX-size cylindrical samples with length to diameter ratio of 2.5 were prepared from the blocks for the uniaxial compressive strength test. However, cubic specimens with  $7 \times 7 \times 7$  cm dimensions were used for the determination of unit weight, effective porosity, water absorption, and sonic velocity. Additionally, direct shear test was carried out along saw-cut surfaces of the rock.

The effective porosity and unit weight tests were performed following buoyancy and saturation technique of ISRM (1981). For the tests, the cubic samples were dipped in water under a vacuum pressure not exceeding 800 Pa for a period of at least 1 h. Saturated

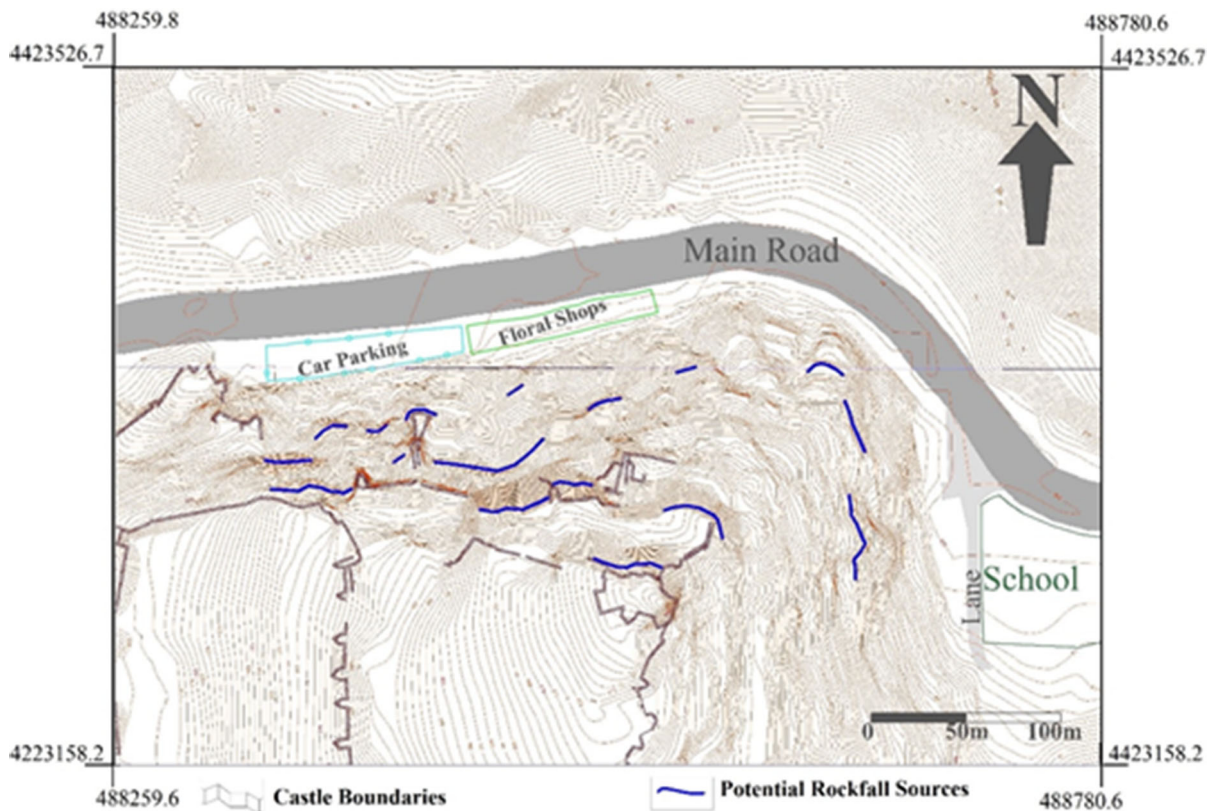


**Fig. 7** Potential rockfall sources in the study area

submerged and saturated-surface dry masses of the andesite samples were then measured. The samples were dried to constant mass at a temperature of 105 °C and then allowed to cool for 30 min in a desiccator before measuring dry mass of the rock. For the water absorption tests, the method proposed in TS 699 (2009) was used. The water absorption of the cubic samples were calculated after 24 h of saturation under atmospheric pressure. The sonic velocity test is a commonly used method which measures the velocity of elastic waves in rocks (ISRM 1981). Saturated and dry sonic velocities of the andesite samples having smooth and flat end surfaces were tested using ultrasonic pulse method. The surface of the 54 kHz transducers is covered with a thin vaseline material in this study. Pulse transmission technique was preferred for the sonic velocity test. In this method, the transmitter and receiver were put on the opposite sides of the tested samples. For the uniaxial compressive strength (UCS) test, dry and saturated NX-size cylindrical specimens having length to diameter ratio

of 2.5 were used. The test was performed on seven samples for each case. During the tests, the load with a constant stress rate of 0.5–1 MPa/s is applied (ISRM 1981). The maximum load at the time of failure was considered to calculate UCS of the rock. In order to achieve shear strength parameters of the discontinuities, Barton–Bandis method which requires determination of the  $\phi_{\text{basic}}$  of the saw-cut surfaces of the rock (Barton and Bandis 1990) was used. Direct shear tests were performed according to ISRM (1981) on three saw-cut andesite surfaces with an instrument applying a constant normal stress and shear stress measurements with displacements less than 0.5 mm/min. Based on the data collected, both peak and residual basic shear strength parameters of the saw-cut surface of the andesite material were calculated. These values and other discontinuity properties (joint wall compressive strength—JCS and joint roughness coefficient—JRC) were then utilized to determine shear strength of the discontinuities for kinematic and limit

**Table 1** Laboratory test results for the andesite

Properties	Standard used for testing	Number of tests	Andesite mean $\pm$ SD
Effective porosity (%)	ISRM (1981)	18	8.2 $\pm$ 1.31
Dry unit weight (kN/m <sup>3</sup> )	ISRM (1981)	18	22.20 $\pm$ 0.45
Saturated unit weight (kN/m <sup>3</sup> )	ISRM (1981)	18	23.01 $\pm$ 0.51
Water absorption under atmospheric pressure- by weight (%)	TS 699 (2009)	18	3.50 $\pm$ 0.55
Dry sonic velocity <sup>a</sup> (m/s)	ISRM (1981)	9	2154.99 $\pm$ 544.49
Saturated sonic velocity <sup>a</sup> (m/s)	ISRM (1981)	9	3367.60 $\pm$ 319.18
Dry uniaxial compressive strength (MPa)	ISRM (1981)	7	46.03 $\pm$ 4.79
Saturated uniaxial compressive strength (MPa)	ISRM (1981)	7	31.47 $\pm$ 11.20
Cohesion <sup>b</sup> (kPa)	ISRM (1981)	3	32.81
Internal friction angle— $\phi_{\text{basic}}$ <sup>b</sup> (°)	ISRM (1981)	3	28.2

SD standard deviation

<sup>a</sup>Pundit plus 54 kHz transducers are used

<sup>b</sup>Shear strength values for saw cut surfaces

equilibrium analyses of the discontinuity-controlled slopes.

The test results are provided in Table 1. The laboratory results indicate that the effective porosity of the andesite ranges between 6.79 and 10.86% with an average effective porosity of 8.2%. The effective porosity and density of the rock correspond to the medium category of Anon (1979). The rock belongs to moderately strong category of ISRM (1981, 2007). The sonic velocity of the rock falls in low to very low and medium to low category (Anon 1979). Very low velocity values, especially in dry conditions, are attributed to the occurrence of micro-fractures which can be developed during cooling of the andesite. Low cohesion values (but not zero) obtained from the direct shear testing is attributed the surface properties which are not totally smooth due to the random distribution of the minerals on the saw-cut rock surface (San 2017).

## 4 Slope Stability Analyses

### 4.1 Kinematic Analyses

In case persistent discontinuities intersect each other in a rock mass, kinematic analyses provide useful information related to the types of discontinuity-controlled rock slope failures. Kinematic analyses were finalized by Dips v.6 software to define whether or not planar, wedge and toppling failures are probable

for the study area (Rocscience 2015a). The analyses were carried out at all 21 stops separately with the discontinuity data measured through the scanline surveys (Table 2). Internal friction angle of the discontinuities was determined by (Barton and Bandis 1990) equation considering basic friction angle, joint roughness coefficient (JRC) and joint wall compressive strength (JCS). The basic friction angle was, however, obtained from the direct shear test performed on the saw-cut surfaces. JRC was measured in the field with hand profilometer (San 2017). JCS was measured with the Schmidt rebound hammer and converted to UCS by using the chart of Deere and Miller (1966). Following the procedure explained in Wyllie and Mah (2004), JRC<sub>n</sub> and JCS<sub>n</sub> with scale effect correction were determined. The slope angle at each stop was considered to evaluate the potential failure modes in the andesite. The analyses for the 10th stop as an example are presented in Fig. 8. According to the analyses, the wedge failure is expected to occur at all stops. However, the planar failure is likely to occur at all stops with exception of 5th, 12th, 13th, 14th, 19th and 21th stops. On the other hand, the toppling failure is expected to happen in most of the stops, excluding 12th, 13th, 19th and 20th ones.

### 4.2 Limit Equilibrium Analyses

By considering the failure modes from the kinematic evaluations, limit equilibrium analyses were

**Table 2** Kinematic failure results for all the stops in the study area

Stops	Kinematic failure types		
	Planar	Wedge	Toppling
1	+	+	+
2	+	+	+
3	+	+	+
4	+	+	+
5	–	+	+
6	+	+	+
7	+	+	+
8	+	+	+
9	+	+	+
10	+	+	+
11	+	+	+
12	–	+	–
13	–	+	–
14	–	+	+
15	+	+	+
16	+	+	+
17	+	+	+
18	+	+	+
19	–	+	–
20	+	+	–
21	–	+	+

performed to assess the stability of the critical slopes. RocPlane 3.0 (Rocscience 2015b), Swedge 6.0 (Rocscience 2015c) and RocTopple 1.0 (Rocscience 2015d) softwares were used to find the safety factors of the planar, wedge and toppling failures, respectively. Static and dynamic conditions were considered during the analyses. The parameters considered during the limit equilibrium analyses are presented in Table 3. The unit weight of the rock was measured by the laboratory test. The Barton–Bandis shear strength model was taken the input data.  $\phi$ basic of the saw-cut surface of the rock was obtained from the internal friction angle of the direct shear test. JRC and JCS were assessed in the field and corrected for scale effect with the procedure explained in Wyllie and Mah (2004). Based on the field observations, slope heights of 10 m and upper slope face angle of 2° were considered in the analyses.

Factor of safety values of the slopes for wedge, planar and toppling failures under static conditions are provided in Table 4. Most of the safety factors except wedge failures of 3rd and 7th stops, and toppling failure of 10th stop, are very low. By considering the seismicity of Ankara region with the North Anatolian Fault as the main seismic source (Teoman et al. 2004), peak ground acceleration was taken as 0.05 g for dynamic conditions. A slight decrement of the factor of safety values of the slopes is evident for the dynamic conditions due to the adverse effect of seismic accelerations on the slope stability. Factor of safety of the slopes for wedge, planar and toppling failures under the dynamic conditions are presented in Table 4. The results of the limit equilibrium analyses reveal that rock failures in several stops may occur in both static and dynamic conditions. Furthermore, the unstable blocks are ready to go into rockfall mode after discontinuity-controlled failure. After conducting the dynamic limit equilibrium analyses by applying horizontal seismic ground acceleration of 0.05 g, the safety factor values of the failures became lower than the static analyses.

### 4.3 Evaluation of the Rockfall Risk

The assessment of rockfall risks along roads and/or settlement places is of great importance for rockfall-related problems (Budetta 2004). Therefore, the rockfall risk of the study area was assessed based on the methodology developed by Saroglou et al. (2012) and suitable for historical sites. In this hazard system, first category of hazard, category A, involves parameters of the geometry of the slope (angle, height, slope roughness and vegetation) and height of the rockfall areas. Category B parameters state to the rock mass and geological conditions of the slope, and Category C parameters associated with the potential triggering factors (rainfall, seismicity of the area) and drainage conditions of groundwater. The categories and their weights in the total risk score are given in Table 5. A slope with the highest risk has a total weighted score of 100 in a 1–100 scale. The parameters of each category, the weight factor for each parameter and their ratings for the study area are depicted in Table 6. Based on the rating method, the total weighted score for the study area is calculated as 49.9 that can be considered as medium scale risk with light remedial measures such as bolts, nets, simple light fences and removal of

**Fig. 8** Kinematic analysis of the 10th stop for **a** planar, **b** wedge, and **c** toppling failures

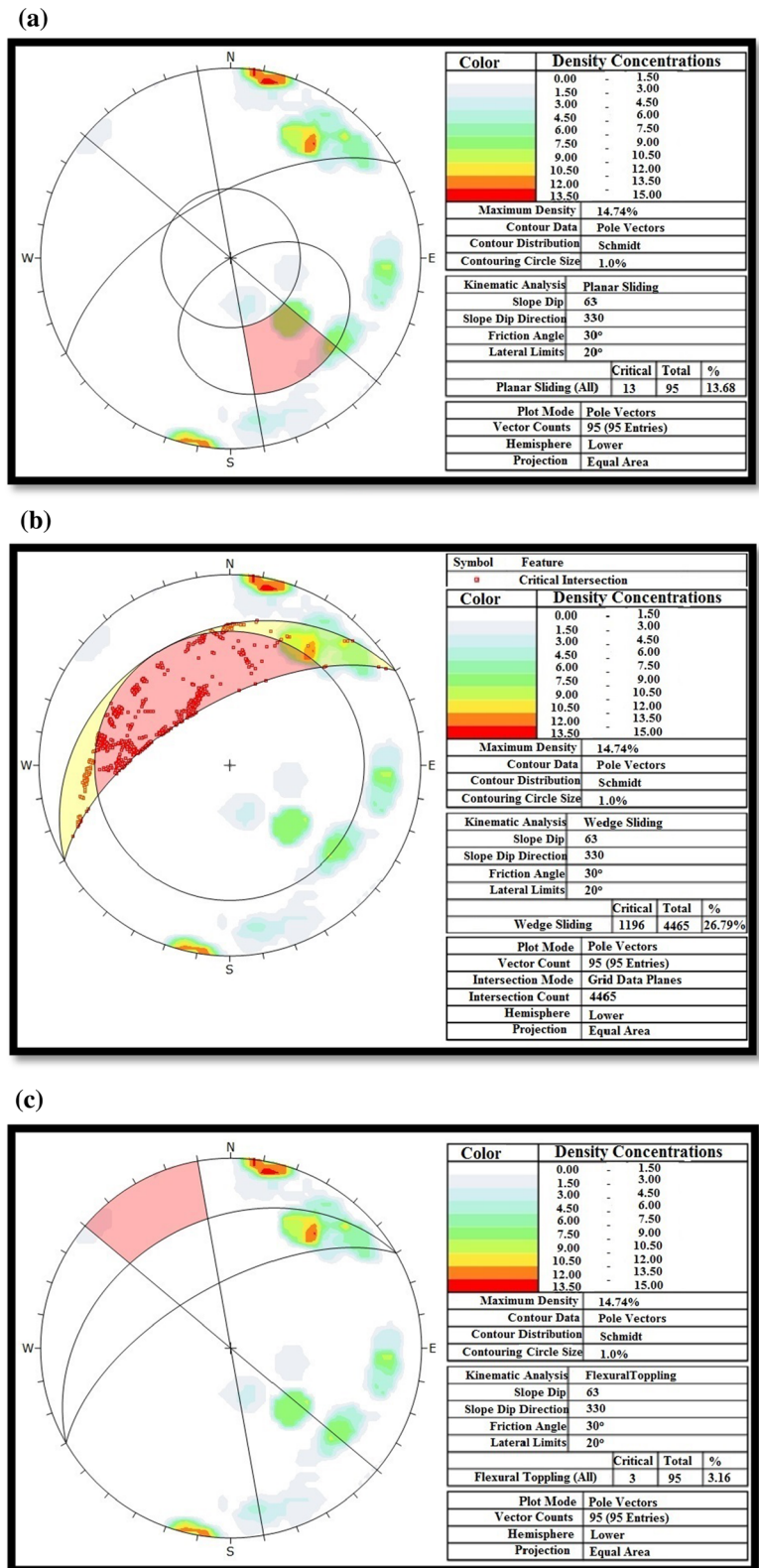


**Table 3** Parameters used in the limit equilibrium analyses

Parameters	Value
Unit weight	22.88 kN/m <sup>3</sup>
$\varphi_{\text{basic}}$	28.2°
JRC <sub>n</sub>	3.28 <sup>a</sup>
JCS <sub>n</sub>	3.55 MPa <sup>a</sup>
Slope height	10 m
Upper face angle	2°

<sup>a</sup>Value after scale effect correction

unstable blocks. These findings, except the use rock bolt, are compatible with the rockfall analyses and field evaluations.

#### 4.4 Rockfall analyses

Regarding rockfall models, two main categories namely lumped-mass and rigid-body exist. In

lumped-mass simulations, the models simplify the calculation models by ignoring the size and shape of the block, and they model the block’s mass as a concentrated single point. However, in rigid-body methods, they take into account the size and shape of the rock block. Newtonian mechanical principles are used with evaluating of translational and rotational velocities of the rockfall blocks and the corresponding energies. Simulation models using rigid-body generally are more capable of accurately reproducing rockfall trajectories that involve all modes of the rockfall phenomenon such as free fall, bouncing, rolling and sliding (TRB 2012).

2D rockfall analyses were performed with RocFall 5.0 (Rocscience 2015e). RocFall is powerful and user-friendly software to simulate rockfall events. It utilizes a particle analysis to evaluate the movement of the rock (Stevens 1998). Compared to the older versions of the program, it considers the shape of the rocks into impact calculations with the rigid body formulation.

**Table 4** Safety factor values obtained from the limit equilibrium analyses for static and dynamic conditions

Stop #	Factor of safety values					
	Planar		Wedge		Toppling	
	Static	Dynamic	Static	Dynamic	Static	Dynamic
1	0.893	0.808	0.293	0.252	0.467	0.458
2	0.209	0.170	0.228	0.186	0.668	0.662
3	0.659	0.598	1.132	1.025	0.760	0.736
4	0.438	0.391	0.658	0.594	0.844	0.732
5	–	–	0.886	0.803	0.364	0.342
6	0.312	0.270	0.956	0.861	0.526	0.494
7	0.201	0.161	1.169	1.061	0.634	0.359
8	0.147	0.106	0.407	0.360	0.436	0.435
9	0.088	0.047	0.402	0.355	0.490	0.486
10	0.909	0.822	0.520	0.465	1.410	0.491
11	0.181	0.142	0.451	0.396	0.391	0.390
12	–	–	0.996	0.902	–	–
13	–	–	0.445	0.388	–	–
14	–	–	0.354	0.306	0.536	0.536
15	0.133	0.092	0.475	0.424	0.493	0.190
16	0.469	0.422	0.154	0.109	0.538	0.345
17	0.360	0.316	0.880	0.779	0.483	0.440
18	0.370	0.326	0.471	0.410	0.459	0.439
19	–	–	0.842	0.772	–	–
20	0.300	0.258	0.864	0.783	–	–
21	–	–	0.407	0.360	0.362	0.347

**Table 5** The categories and their weights in the total risk score (Saroglou et al. 2012)

Risk Class	Total weighted score 1–100	Risk	Indicative protection measures (the choice is site specific)
I	< 20	Very low	Not necessary. May be sparse spot interventions
II	21–40	Low	In limited extent
III	41–60	Medium	Light measures (such as bolts, nets, removal of unstable blocks, simple light fences)
IV	61–80	High	Combination of active (such as bolts, anchors) and passive (such as nets, wire rope cables, buttress walls, fences removal of unstable blocks) measures
V	81–100	Very high	Critical state of stability, combination of generalized or/and strong active and passive measures. Residual risk to be accepted

**Table 6** Risk rating system results for the study area

Category	Parameter	Point	Score
A	1. Slope angle (°)	100	7
	2. Slope height (m)	10	0.4
	3. Release area height	60	4.2
	4. Slope roughness	30	0.9
	5. Vegetation of slope	100	4
B	6. Joint roughness/filling material in joints/Joint opening	30	1.8
	7. Joint orientation	30	1.5
	8. Joint persistence	60	2.4
	9. Joint compressive strength	10	0.1
	10. Strength of intact rock	60	0.6
	11. Block volume	15	0.6
	12. Estimated number of blocks	60	1.2
	13. Karstic features	10	0.2
C	14. Rainfall	30	0.9
	15. Permeability	15	0.45
	16. Seismicity	10	0.4
D	17. Width of catchment zone (m)	100	10
	18. Rockfall history	15	0.75
	19. Slope accessibility	10	0.5
	20. Potential result of impact	60	12
Total score			49.9
Risk class			Medium

This approach was preferred for the 2D analyses of this study.

Several profiles along steep slopes were chosen in such a way that the problematic areas are entirely covered. The analyses were done along 20 profiles (Fig. 9). More than one potential rockfall sources exist along some of the profiles. The analyses were carried out for each profile from each rockfall source location.

The parameters used in the 2D analyses are given in Table 7. The tangential and normal coefficients of restitution of the andesite were taken as 0.71 and 0.46, individually for the analyses due to similarities of the rock type crops out around Afyon Castle (Topal et al. 2007) and the study area. Due to the fact that the rockfall source area is very close to the road and floral shops, back analysis to ascertain normal and tangential

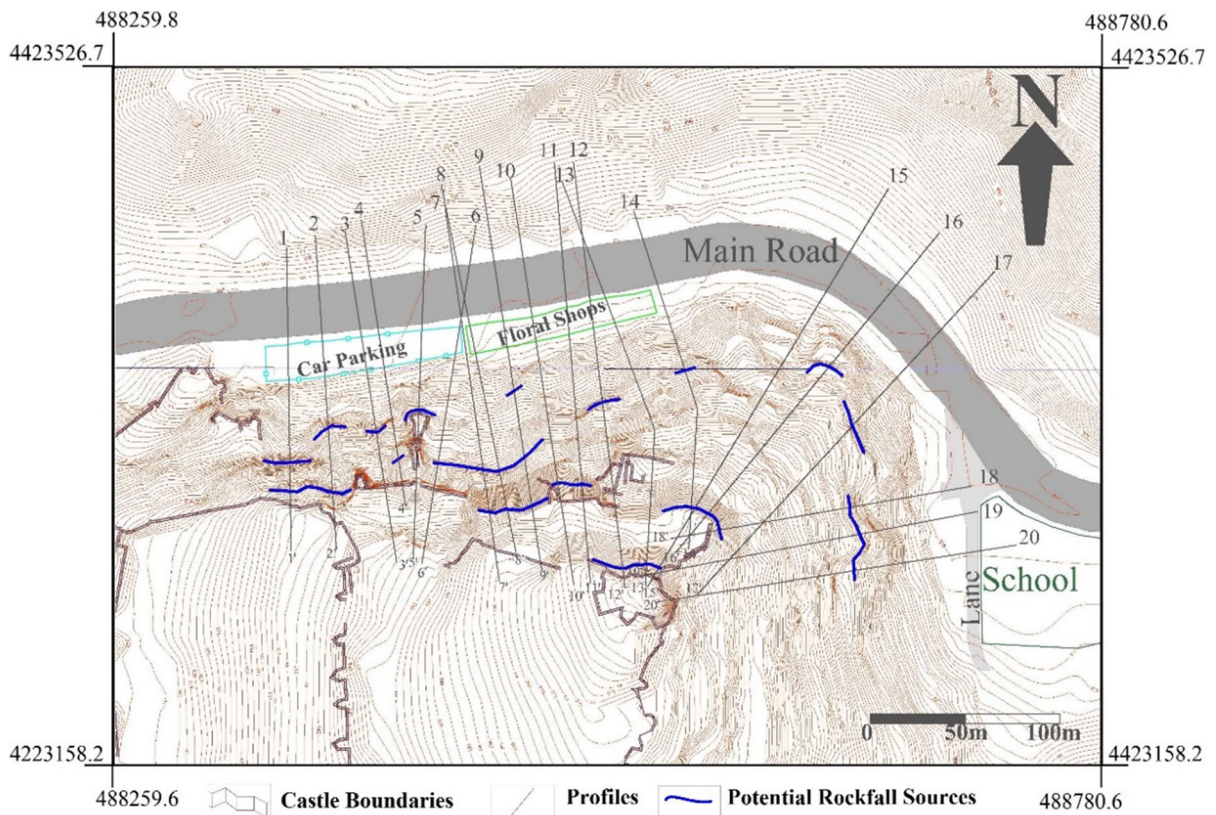


**Fig. 9** Profiles used for 2D rockfall analyses. Rockfall source areas are shown by blue color

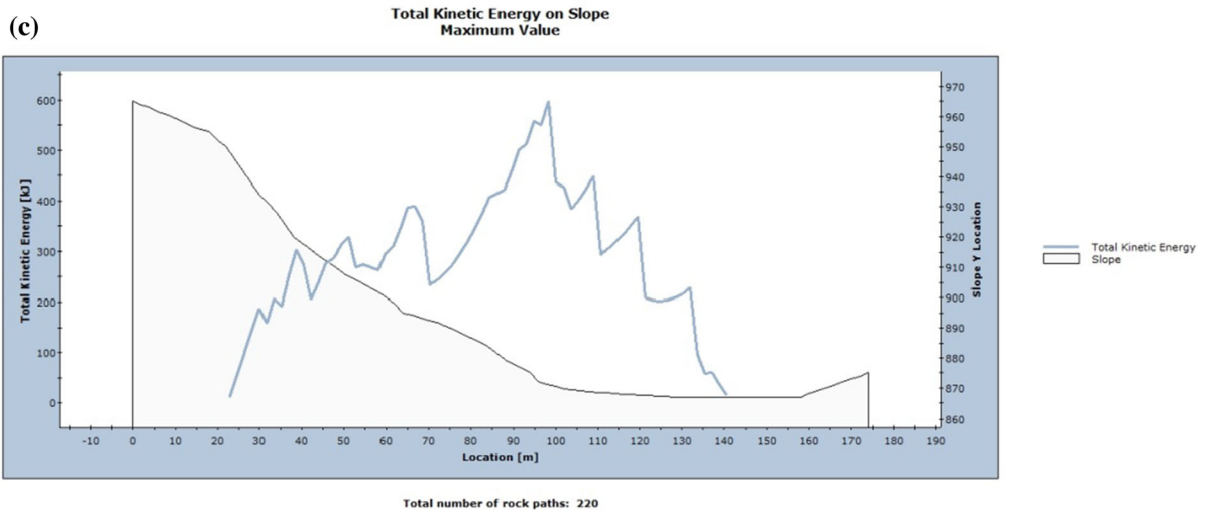
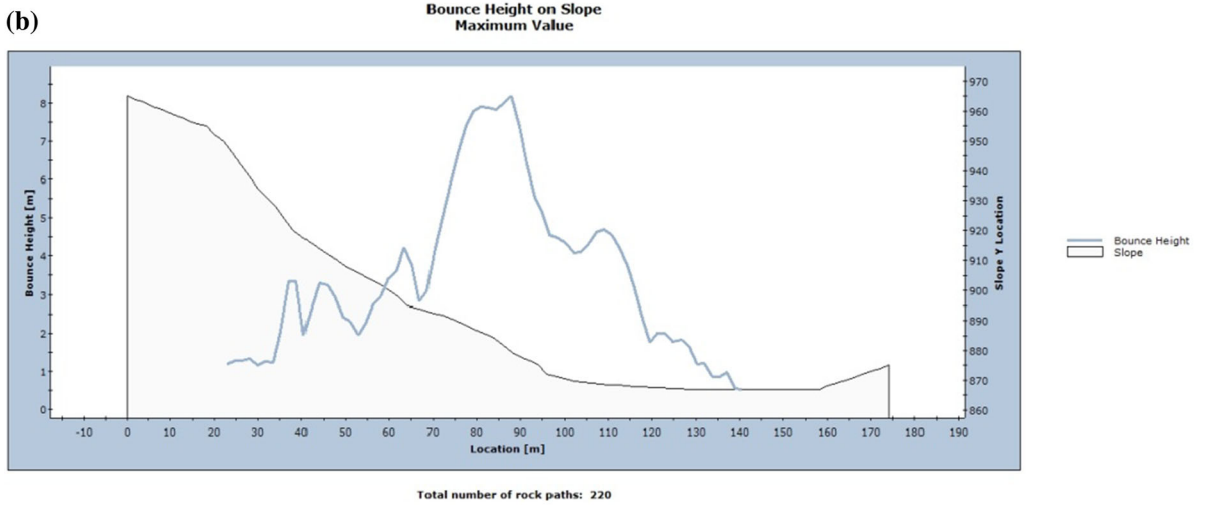
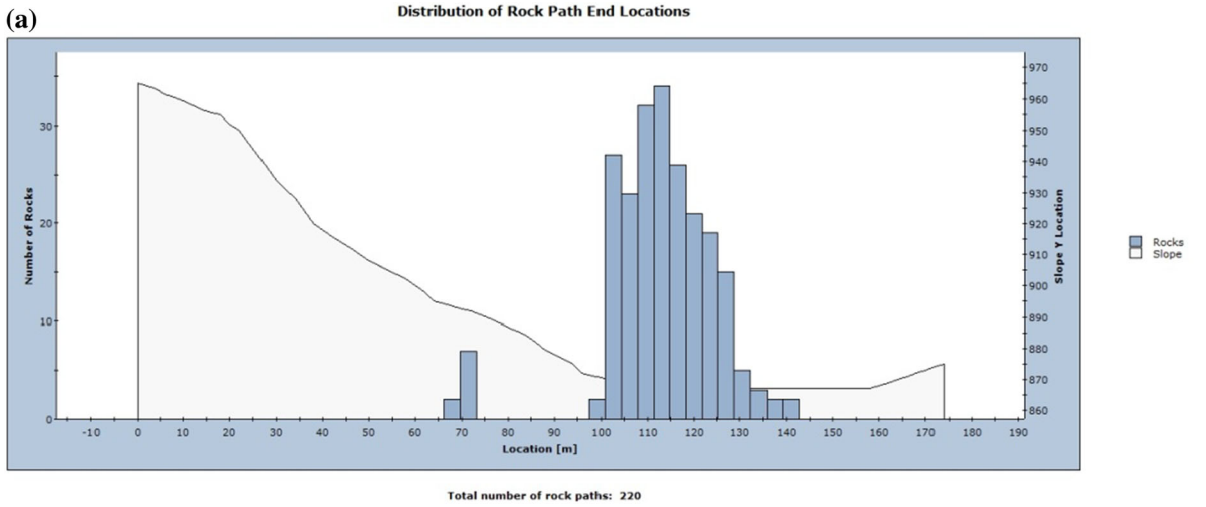
**Table 7** Parameters used for 2D rockfall analyses

Parameters	Value
Normal coefficient of restitution	0.46 ± 0.05
Tangential coefficient of restitution	0.71 ± 0.05
Dynamic friction coefficient	0.58 ± 0.04
Rolling resistance	1.31 ± 0.02
Initial velocity (m/s)	1
Number of throws	1000 rocks
Minimum velocity cut-off (m/s)	0.1
Shape of the rocks thrown	Hexagonal

coefficients of restitution ( $R_n$  and  $R_t$ ) could not be performed in the field. As an initial velocity, 1 m/s was selected for long-term rockfall conditions due to the importance of the site properties (touristic/historical area), geological and seismicity conditions, and urbanization. However, the dynamic friction coefficient parameter calculated as tangent of the

international friction angle,  $\tan(\phi)$  (Rocscience 2015e) was taken as 0.58, whereas the internal friction angle for rockfall analyses was obtained from a field test on the andesite of the Afyon Castle (Topal et al. 2007). Moreover, back analysis was carried out in RocFall v.5 by using the largest fallen block in the study area to acquire the value of rolling resistance. The rockfall source areas and block locations were assessed from the field study. For this reason, the rocks were thrown in the software along 3–3' profile with different rolling resistance values from the range of the values provided by Rocscience (2015e). Thus, a rolling resistance of about 1.31 was obtained for the study area (San 2017).

Rocks with different weights (250 kg, 500 kg, 750 kg and 1800 kg) representing the site condition were thrown using the software. As the results of the 2D analyses, run-out distance, total kinetic energy, bounce height values were achieved for every profile and rockfall source. Typical graphs of end point, bounce height and total kinetic energy values are



◀ **Fig. 10** Typical graphics of 2D analyses results along profile 9'–9: **a** end point location, **b** bounce height, and **c** total kinetic energy

depicted in Fig. 10. The 2D analysis reveal that rockfall mode is generally in the form of bouncing. By using the run-out distances at each profile for each weight of the rocks, danger zones were illustrated separately on the topographic map (Fig. 11). As can be seen from Fig. 11, the worst case is for the danger zone with the heaviest block (1800 kg) used. The 2D rockfall analyses clearly reveal that the road, floral shops, car parking, and small lane are in danger of the rockfall. For this reason, remedial measures should be considered in engineering practice.

### 5 Evaluation of Stability Analyses and Remedial Measures

The limit equilibrium analyses performed around the Ankara Citadel indicate that slopes are mainly unstable and blocks are ready to fall. On the other hand, the rockfall analyses show that there exists rockfall danger zone in northern and eastern part of the Citadel affecting the settlement area.

Within the framework of this study, the rockfall source determined was also compared with rockfall source area (RSA) map (Fig. 12) around the Citadel and its vicinity generated by Aksoy and Ercanoglu (2006). In their study, they collected some discontinuity data for a large area, including the Citadel. They stated that rockfall initiation is in relation with discontinuity characteristics and natural slope. The mean spacing of the discontinuities was found to be

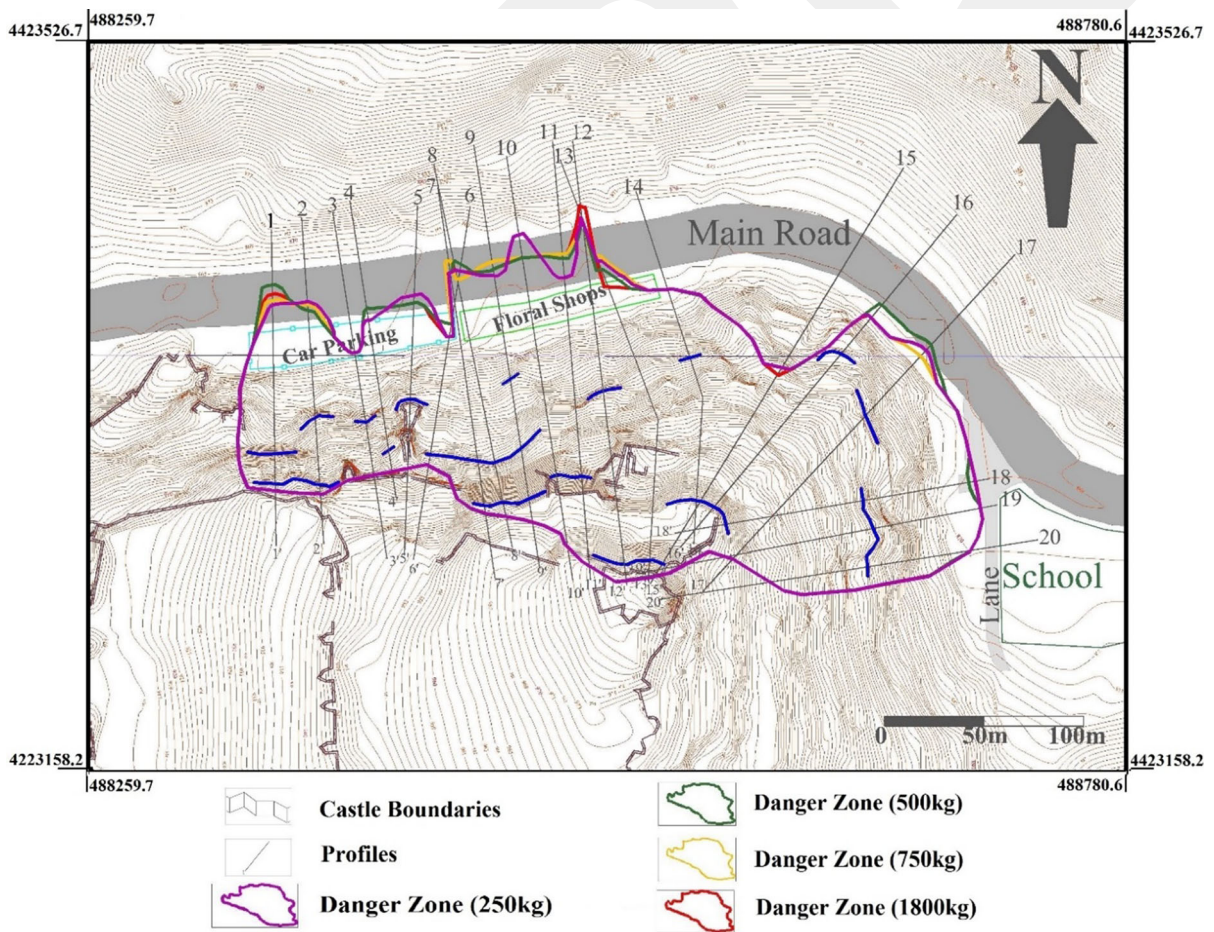


**Fig. 11** Danger zones assessed from the 2D analyses with the rocks of different weights

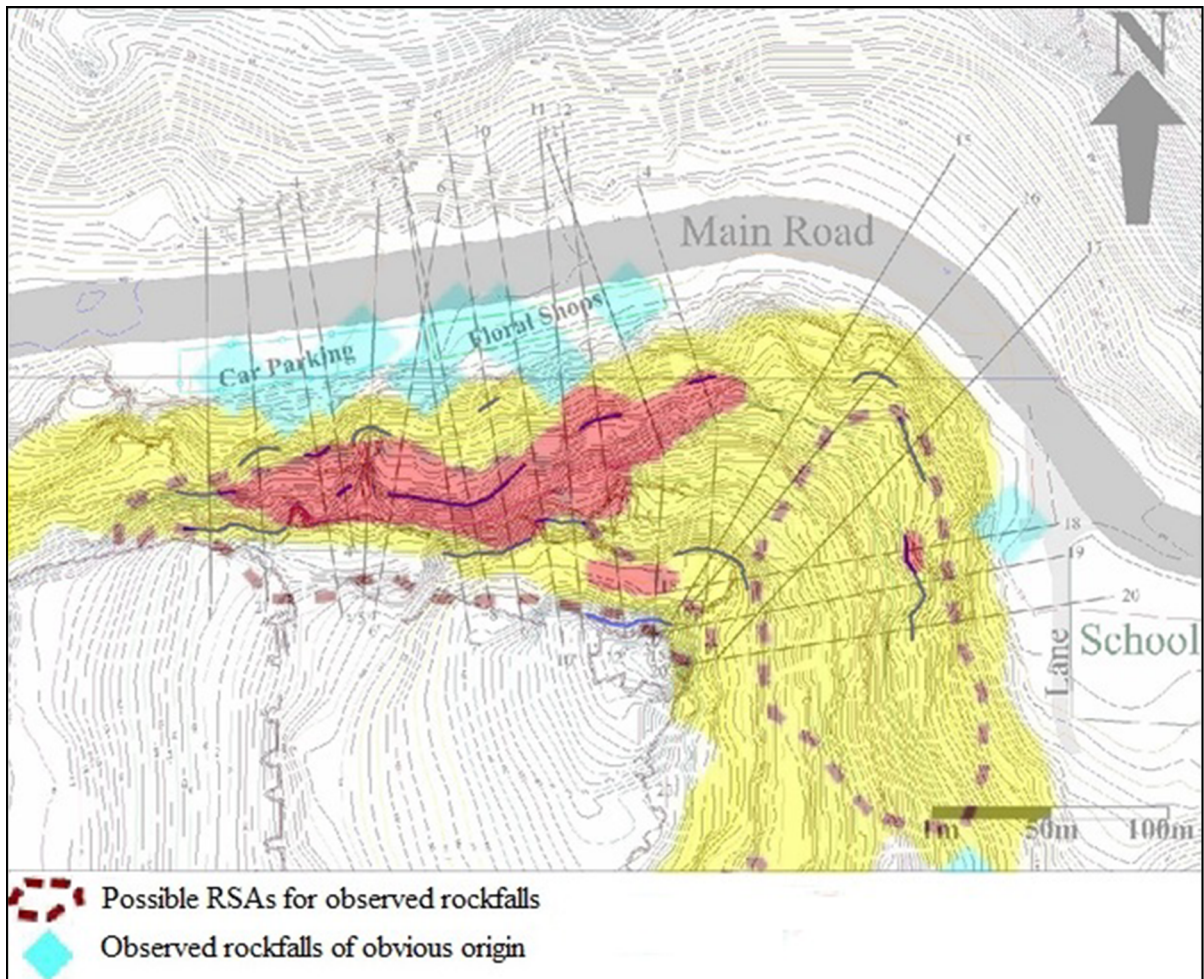


**Fig. 12** RSA map around the Ankara Citadel and its vicinity generated by Aksoy and Ercanoglu (2006). The yellow and red areas represent medium and high rockfall source areas, respectively

ranging between 0.21 and 0.39 m. These values correspond to lower limit of our measurements. Altitude difference, number of discontinuities, number of potential sliding, and number of wedges were considered as input parameters of the rule-based fuzzy system on the basis of the data availability and engineering judgment. These parameters were processed in the fuzzy system to get an output (i.e. degree of being RSA). Aksoy and Ercanoglu (2006) also observed some rockfall problems around the Citadel. In Fig. 12, the blue diamond shapes show the rockfalls already observed in the related study. However, the dash line areas indicate the possible rockfall sources determined by Aksoy and Ercanoglu (2006). These authors stated that most of the rockfall sources assessed in their study area are found to be in medium

rockfall source area and locally in high rockfall source area. However, the rockfall source area near the inner circle of the Caste, which was found in our study, was not included in the RSA map. The run-out distances from this source area reach the most distant locations through the profiles 12 and 13 in the rockfall analysis, whereas the shortest run-out distance is also from this rockfall source area, but through the profile 15.

Due to the presence of the floral shops and car parking area at the lower level of the hill, construction of ditches is not considered to be attainable without giving disturbances to the surrounding area. Furthermore, rock bolt installations are not also practical because the discontinuity spacing is generally very low. The design of the rock bolts' size would be very difficult to establish due to the limitation of the

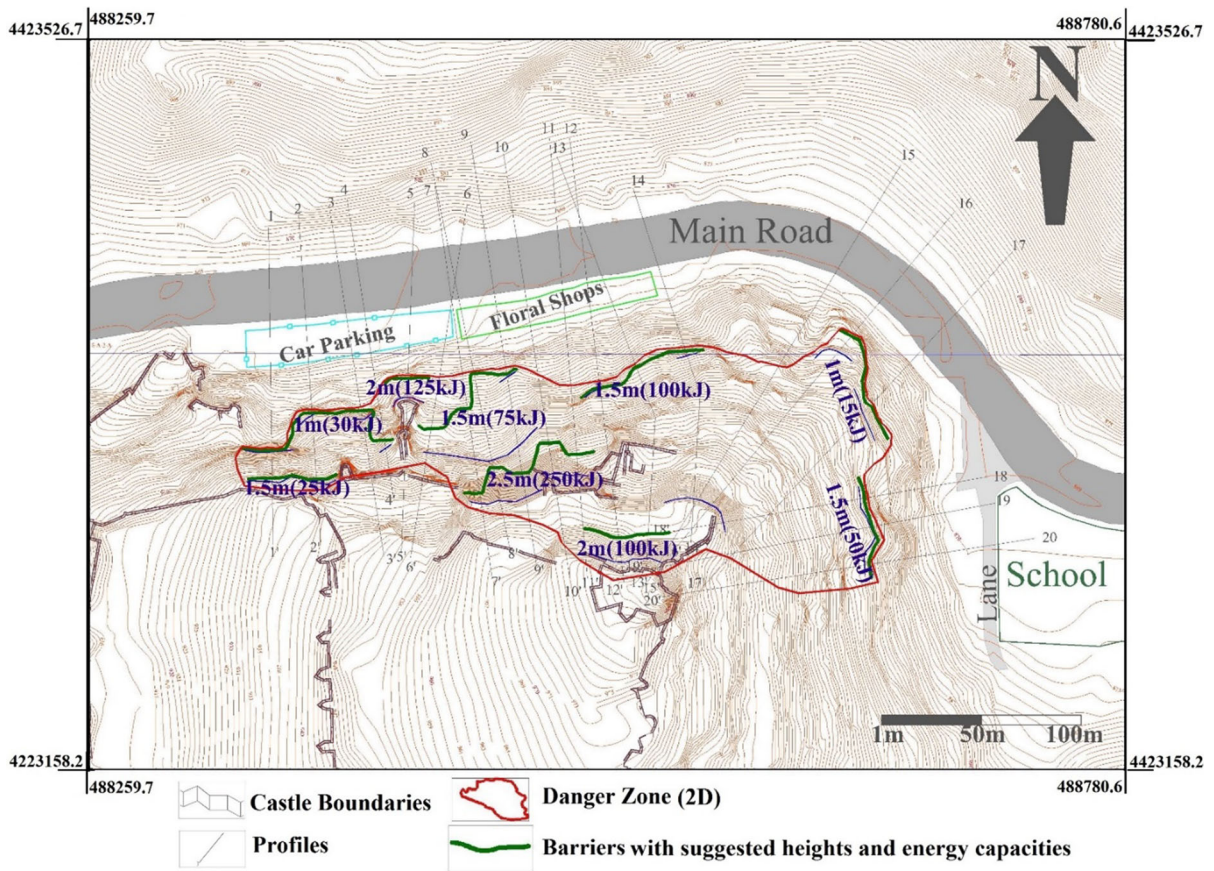


**Fig. 13** Design for installation of barriers on the slope to prevent rockfall damage in the study area

discontinuity persistence caused by the flow character of the andesite. The rockfall-prone zone also covers a large area requiring too many bolts. Therefore, as the first step of remediation, the loose andesite blocks already to detach should be cleaned since those unstable blocks may fall down at any time. Catch barriers are recommended to terminate the andesite blocks from reaching down the road as an effective method of protection. The impact energy and fall trajectories are needed to confirm strength, height and location of the barriers on the slope for the rockfall protection design (Wyllie 2015; Li et al. 2016). These design parameters were obtained from RocFall v.5 (Rocscience 2015e) in this study. For each profile, the characteristics of the trajectories such as bounce height, impact energy, and run-out distance were investigated. The location, height and energy capacities of the barriers were determined in such a way that cost-effective solution with relatively short height and low capacity of the barriers can be used. The rockfalls

were simulated using the software by installing the barriers to make sure that they stop the falling block. Therefore, barriers of various sizes (from 1 to 2.5 m height with and 15 to 250 kJ capacities) were selected at different locations. The most suitable catch barriers suggested are shown in Fig. 13. The rockfalls were simulated again by adding the catch barriers along the profiles, and it is observed that the infrastructures are not adversely affected even from the worse rockfall events (Fig. 13).

### 6 Conclusions

The Ankara Citadel is located on a very steep hill. There are floral shops, main road, car parking and a school near the lower part of the hill. The highly fractured andesite is the main geological unit in the area and is mainly pinkish grey and dominantly slightly to moderately weathered.

Detailed scanline surveys conducted at 21 stops in the study area reveal that several steeply dipping cooling joints developed in different directions nearly perpendicular to the flow layers. Many fallen andesite blocks were seen in the field that reached near to the main road and floral shops. This study indicates that slopes are unstable and rockfall events are expected to occur especially on the eastern and northern parts of the hill.

As the result of kinematic analyses of each stop of the study area, the wedge failure is likely to happen at all the stops. The planar failure is expected to happen at all the stops except 5th, 12th, 13th, 14th, 19th and 21th stops. The toppling failure is probable to occur in most stops, excluding 12th, 13th, 19th and 20th stops. The safety factors of all failure types in static limit equilibrium analyses are very low under 1.0 except wedge failure of 3rd and 7th stop, and toppling failure of 10th stop. 2D rockfall analyses along 20 profiles, which were carried out with four different weights of the rocks such as 250 kg, 500 kg, 750 kg and 1800 kg revealed that the fallen rocks may reach to the main road, car parking, floral shops and the school. Comparison of 2D and 3D rockfall analyses showed that the runout distances of 3D analyses are further than those of 2D analyses. Different results were given by those two analyses due to rockfall models, algorithms used and the parameters input. However, based on the restriction of 2D analysis for the rockfall track, 3D results are accepted to be more authentic.

Removal of the detached and loosen andesite blocks is suggested with annual periodic control because the neighborhood is not suitable to relocate. Furthermore, catch barriers installations on the slope with specified heights, energy capacities and locations are also recommended to save the surrounding area. Depending on the results of the proposed rockfall risk classification system, the weighted score corresponds to medium risk category that can be grouped in the light remedial measures for the indicative protection of the study area.

**Acknowledgements** The authors gratefully acknowledge Altındag Municipality for the topographical data of the study area. We are also indebted and thankful to Rocscience Company for allowing the access of the software related to various slope stability analyses. The authors would like to express gratitude to Yavuz Kaya and Timur Ersöz for their help during the field study.

## References

- Agliardi F, Crosta GB (2003) High resolution three-dimensional numerical modelling of rockfalls. *Int J Rock Mech Min Sci* 40:455–471
- Agliardi F, Crosta GB, Frattini P (2009) Integrating rockfall risk assessment and countermeasure design by 3D modelling techniques. *Nat Hazards Earth Syst Sci* 9:1059–1073
- AFAD (1996) Earthquake zoning map of Turkey. Prime Ministry Disaster and Emergency Management Authority of Turkey, Earthquake Research Department, Ankara
- Aksoy H, Ercanoglu M (2006) Determination of the rockfall source in an urban settlement area by using a rule-based fuzzy evaluation. *Nat Hazards Earth Syst Sci* 6:941–954
- Akyürek B, Duru M, Sütçü Y, Papak I, Şaroğlu F, Pehlivan N, Gönenç O, Granit S, Yaşar T (1997) 1:100000 scaled geological map of Turkey. Ankara - F15 plate, MTA Press, Ankara
- Aqeel AM (2018) Rockfall Hazard Rating System(s) in Saudi Arabia – A Review. *J Geogr Geol* 10(4)
- Anon (1979) Classification of rocks and soils for engineering geological mapping. Part 1. Rock and soil materials. *Bull Int Assoc Eng Geol* 19:364–371
- Ansari MK, Ahmad M, Singh R, Singh TN (2018) 2D and 3D rockfall hazard analysis and protection measures for Saptashrungi Gad Temple, Vani, Nashik, Maharashtra—a case study. *J Geol Soc India* 91(1):47–56
- Antoniu AA, Lekkas E (2010) Rockfall susceptibility map for Athinios port, Santorini Island Greece. *Geomorphology* 118(1–2):152–166
- Asteriou P, Tsiambaos G (2018) Effect of impact velocity, block mass and hardness on the coefficients of restitution for rockfall analysis. *Int J Rock Mech Min Sci* 106:41–50
- Azzoni A, Barbera LG, Zaninetti A (1995) Analysis and prediction of rockfalls using a mathematical model. *Int J Rock Mech Min Sci Geotech Abstr* 32:709–724
- Barton N, Bandis S (1990) Review of predictive capabilities of JRC-JCS model in engineering practice. In: Barton N, Stephansson O (eds.) *Proceedings of the International Symposium on Rock Joints*, Loen, Norway. Balkema, Rotterdam, pp 603–610.
- Basharat MK, Yasir S (2018) Effects of volume and topographic parameters on rockfall travel distance: a case study from NW Himalayas. *J Eng Geol Hydrogeol* 51:387–398. <https://doi.org/10.1144/qjgegh2017-027>
- Basharat M, Rohn J, Ehret D, Baig MS (2012) Lithological and structural control of Hattian Bala rock avalanche triggered by the Kashmir earthquake 2005, Sub-Himalayas, Northern Pakistan. *J Earth Sci* 23(2):213–224
- Basharat M, Rohn J, Baig MS, Khan MR, Schleier M (2014) Large scale mass movements triggered by the Kashmir earthquake 2005 Pakistan. *J Mt Sci* 11(1):19–30
- Bigot C, Dorren L, Berger F (2009) Quantifying the protective function of a forest against rockfall for past, present and future scenarios using two modelling approaches. *Nat Hazards* 49:99–111
- Binal A, Ercanoglu M (2010) Assessment of rockfall potential in the Kula (Manisa, Turkey) geopark region. *Environ Earth Sci* 61(7):1361–1373

- Bourrier F, Dorren L, Nicot F, Berger F, Darve F (2009) Toward objective rockfall trajectory simulation using a stochastic impact model. *Geomorphology* 110:68–79
- Bozzolo D, Pamini R, Hutter K (1988) Rockfall analysis—a mathematical model and its test with field data. In: *Proceedings of the 5th international symposium on landslides, Lausanne* 1 pp. 555–560
- Budetta P (2004) Assessment of rockfall risk along roads. *Nat Hazards Earth Syst Sci* 4(1):71–81
- Budetta P (2010) Rockfall-induced impact force causing a debris flow on a volcanoclastic soil slope: a case study in southern Italy. *Nat Hazards Earth Syst Sci* 10:1995–2006
- Chau KT, Wong RHC, Lee CF (1998) Rockfall problems in Hong Kong and some new experimental results for coefficients of restitution. *Int J Rock Mech Min Sci* 35:662–663
- Chau KT, Wong RHC, Liu J, Lee CF (2003) Rockfall hazard analysis for Hong Kong based on rockfall inventory. *Rock Mech Rock Eng* 36:383–408
- Chen H, Chen RH, Huang T (1994) An application of an analytical model to a slope subject to rockfalls. *Bull Assoc Eng Geol* 31:447–458
- Chen G, Zheng L, Zhang Y, Wu Y (2013) Numerical Simulation in Rockfall Analysis: A Close Comparison of 2-D and 3-D DDA. *Rock Mech Rock Eng*. <https://doi.org/10.1007/s00603-012-0360-9>
- Chiessi V, D'Orefice M, Muggonza GS, Vitale V, Cannese C (2010) Geological, geomechanical and geostatistical assessment of rockfall hazard in San Quirico Villace (Abruzzo, Italy). *Geomorphology* 119(3–4):147–161
- Choi Y, Lee JY, Lee J, Park HD (2009) Engineering geological investigation into rockfall problem: a case study of the Seated Seokgayeorae image carved on a rock face at the UNESCO world heritage site in Korea. *Geosci J* 13(1):69–78
- Christen M, Bartelt P, Gruber U (2007) RAMMS—A modelling system for snow avalanches, debris flows and rockfalls based on IDL. *Photogramm Fernerkund Geoinf* 4:289–292
- Chun Z, Zhigang T, Sen Y, Shuai Z (2018) V shaped gully method for controlling rockfall on high-steep slopes in China. *Bull Eng Geol Environ* 78(4):2731–2747
- Copons R, Vilaplana JM, Linares R (2009) Rockfall travel distance analysis by using empirical models (Sol'a d'Andorra la Vella, Central Pyrenees). *Nat Hazards Earth Syst Sci* 9:2107–2118
- Corominas J, Copons R, Moya J, Vilaplana JM, AltimirAmigó JJ (2005) Quantitative assessment of the residual risk in a rockfall protected area. *Landslides* 2(4):343–357
- Crosta GB, Agliardi F (2003) A methodology for physically-based rockfall hazard assessment. *Nat Hazards Earth Syst Sci* 3:407–422
- Crosta GB, Agliardi F (2004) Parametric evaluation of 3D dispersion of rockfall trajectories. *Nat Hazards Earth Syst Sci* 4:583–598
- Deere DU, Miller RP (1966). Engineering classification and index properties for intact rocks. Technical Report Air Force Weapons Laboratory, New Mexico, No AFWL-67-144.
- de Almeida JA, Kullberg JC (2011) Rockfall hazard and risk analysis for Monte da Lua, Sintra Portugal. *Nat Hazards* 58(1):289–310
- Development and implementation of the Idaho highway slope instability and management system (HiSIMS). National institute for advanced transportation technology, University of Idaho, USA
- Dinçer I, Orhan A, Frattini P, Crosta G (2016) Rockfall at the heritage site of the Tatlarin Underground City (Cappadocia, Turkey). *Nat Hazards* 82(2):1075–1098
- Dorren LKA (2003) A review of rockfall mechanics and modelling approaches. *Prog Phys Geogr* 27:69–87
- Dorren LKA, Maier B, Putters US, Seijmonsbergen AC (2004) Combining field and modelling techniques to assess rockfall dynamics on a protection forest hillslope in the European Alps. *Geomorphology* 57:151–167
- Dorren LKA, Berger F, Putters US (2006) Real-size experiments and 3-D simulation of rockfall on forested and non-forested slopes. *Nat Hazards Earth Syst Sci* 6:145–153
- Erentöz C (1975) 1/15000 scaled geological map of Turkey. MTA Press.
- Erol O (1961) Tectonic development of Ankara region. *Bull TJK* 7:57–85
- Evans SG, Hungr O (1993) The assessment of rockfall hazard at the base of talus slopes. *Can Geotech J* 30:620–636
- Fanos AM, Pradhan B (2019) A novel rockfall hazard assessment using laser scanning data and 3D modelling in GIS. *Catena* 172:435–450
- Fell R, Corominas J, Bonnard C, Cascini L, Leroi E, Savage W (2008) Guidelines for landslide susceptibility, hazard and risk zoning for land use planning. *Eng Geol* 102:85–98
- Ferrari F, Giacomini A, Thoeni K, Lambert C (2017) Qualitative evolving rockfall hazard assessment for highwalls. *Int J Rock Mech Min Sci* 98:88–101
- Franklin JA, Senior SA (1997) The Ontario rockfall hazard rating system. In: *Proceedings of the conference on engineering geology and environment, Athens*, pp 647–658
- Giani GP (1992) *Rock slope stability analysis*. Balkema, Rotterdam
- Gökce O, Özden S, Demir A (2008) Spatial and statistical distribution of disaster in Turkey. *Disaster Information Inventory, Department of Disaster Studies and Damage Assessment, Ankara*
- Guzzetti F, Crosta GB, Detti R, Agliardi F (2002) STONE: a computer program for the three-dimensional simulation of rock-falls. *Comput Geosci* 28:1079–1093
- Guzzetti F, Reichenbach P, Wieczorek GF (2003) Rockfall hazard and risk assessment in the Yosemite Valley, California, USA. *Nat Hazards Earth Syst Sci* 3:491–503
- Gül M, Özbek A, Karacan E (2016) Rock fall hazard assessment in Asar Hill, ancient Mabolla City Mugla-SW Turkey. *Environ Earth Sci* 75(19):1310
- ISRM (1981) Rock characterization, testing and monitoring: ISRM suggested methods. In: Brown ET (ed.) Published for the Commission on Testing Methods. International Society for Rock Mechanics by Pergamon Press, Oxford
- ISRM (2007) The complete ISRM suggested methods for rock characterization, testing and monitoring: 1974–2006. In: Ulusay R, Hudson JS (eds.) Published for the commission on testing methods. International Society for Rock Mechanics by Koçan Ofset, Ankara, Turkey.
- Jaboyedoff M, Dudt JP, Labiouse V (2005) An attempt to refine rockfall hazard zoning based on the kinetic energy,

- frequency, and fragmentation degree. *Nat Hazards Earth Syst Sci* 5:621–632
- Jaboyedoff M, Labiouse V (2011) Preliminary estimation of rockfall runout zones. *Nat Hazards Earth Syst Sci* 11:819–828
- Jaboyedoff M, Oppikofer T, Abellán A, Derron MH, Loye A, Metzger R, Pedrazzini A (2012) Use of LIDAR in landslide investigations: a review. *Nat Hazards* 61(1):5–28
- Katz O, Reichenbach P, Guzzetti F (2011) Rock fall hazard along the railway corridor to Jerusalem, Israel, in the Soreq and Refaim valleys. *Nat Hazards* 56:649–665
- Kaya Y, Topal T (2015) Evaluation of rock slope stability for a touristic coastal area near Kusadasi, Aydin (Turkey). *Environ Earth Sci* 74(5):4187–4199
- Korkanç M, İnce İ, Hatır ME, Tosunlar MB (2018) Historical granaries at Taşkale (Turkey) under risk: a geotechnical analysis. *Mediterr Archaeol Archaeom* 18(1):149–162
- Krautblatter M, Moser M (2009) A nonlinear model coupling rockfall and rainfall intensity based on a four year measurement in a high Alpine rock wall (Reintal, German Alps). *Nat Hazards Earth Syst Sci* 9:1425–1432
- Li LP, Sun SQ, Li SC, Zhang QQ, Hu C, Shi SS (2016) Coefficient of restitution and kinetic energy loss of rockfall impacts. *KSCE J Civ Eng* 20(6):2297–2307
- Maerz NH, Youssef A, Laue, R (2004) MORFH RS: a rock cut rating system for Missouri highways. In: *The 55th highway geology symposium, Kansas City, Missouri, Sep. 7–10, 2004*, pp 406–424.
- Maerz NH, Youssef A, Fennessey TW (2005) New risk-consequence rockfall hazard rating system for Missouri highways using digital image analysis. *Environ Eng Geosci J* 11:229–249
- Maerz NH, Youssef A, Pradhan B, Bulkhi A (2015) Remediation and mitigation strategies for rock fall hazards along the highways of Fayfa Mountain, Jazan Region, Kingdom of Saudi Arabia. *Arab J Geosci* 8(5):2633–2651
- Marzorati S, Luzi L, Amicis MD (2002) Rock falls induced by earthquakes: a statistical approach. *Soil Dyn Earthq Eng* 22:565–577
- Masuya H, Amanuma K, Nishikawa Y, Tsuji T (2009) Basic rockfall simulation with consideration of vegetation and application to protection measure. *Nat Hazards Earth Syst Sci* 9:1835–1843
- Mazzoccola D, Sciesa E (2000) Implementation and comparison of different methods for rockfall hazards assessment in the Italian Alps. In: Glade T, Anderson MG, Crozier MJ (eds) *Proceedings of the 8th international symposium on landslides, Cardiff, UK. Landslide hazard and risk, Vol. 2, Balkema, Rotterdam*, pp. 1035–1040.
- Mineo S, Pappalardo G, Mangiameli M, Campolo S, Mussumeci G (2018) Rockfall analysis for preliminary hazard assessment of the cliff of Taormina Saracen Castle (Sicily). *Sustainability* 10(2):417
- Nicot F, Cambou B, Mazzoleni G (2001) Design of rockfall restraining nets from a discrete element modelling. *Rock Mech Rock Eng* 34:99–118
- New York Department of Transportation (NYDOT) (2007). *Rock slope rating procedure: geotechnical engineering manual GEM-15*. NYDOT, New York.
- O Hungr SG Evans 1988 Engineering evaluation of fragmental hazards. In: *Proceedings of the 5th international symposium on landslides, Lausanne 1*, pp. 685–690
- Okura Y, Kitahara H, Sammori T, Kawanami A (2000) The effects of rockfall volume on runout distance. *Eng Geol* 58:109–124
- Pack R, Boie K, Mather S, Farrell J (2006) UDOT rockfall hazard rating system: final report and user's manual (Report UT-06.07). Utah State University, Logan
- Paronuzzi P (1989) Probabilistic approach for design optimization of rockfall protective barriers. *Q J Eng Geol* 22:175–183
- Peila D, Pelizza S, Sasudelli F (1998) Evaluation of behaviour of rockfall restraining nets by full scale tests. *Rock Mech Rock Eng* 31:1–24
- Peila Ronco DC (2009) Design of rockfall net fences and the new ETAG 027 European guideline. *Nat Hazards Earth Syst Sci* 9:1291–1298
- Pellicani R, Spilotro G, Van Westen CJ (2016) Rockfall trajectory modeling combined with heuristic analysis for assessing the rockfall hazard along the Maratea SS18 coastal road (Basilicata, Southern Italy). *Landslides* 13(5):985–1003
- Perret S, Dolf F, Kienholz H (2004) Rockfalls into forests: Analysis and simulation of rockfall trajectories-considerations with respect to mountainous forests in Switzerland. *Landslides* 1:123–130
- Pierson LA, Van-Vickle R (1993) *Rockfall hazard rating system participant's manual*. SNI International Resources Inc., Phoenix
- Priest SD (1993) *Discontinuity analysis for rock engineering*. Chapman and Hall, London
- Raetzo H, Lateltin O, Bollinger D, Tripet JP (2002) Hazard assessment in Switzerland-code of practice for mass movements. *Bull Eng Geol Environ* 61:263–268
- Rammer W, Brauner M, Dorren LKA, Berger F, Lexer MJ (2010) Evaluation of a 3-D rockfall module within a forest patch model. *Nat Hazards Earth Syst Sci* 10:699–711
- Ritchie AM (1963) Evaluation of rockfall and its control. *Highw Res Board Rec* 17:13–27
- Rocscience (2015a) Dips v.6-graphical and statistical analysis of orientation data. Rocscience Inc., Toronto
- Rocscience (2015b) RocPlane v.3-planar rock slope stability analysis and design. Rocscience Inc., Toronto
- Rocscience (2015c) Swedge v.6-stability of surface wedges in rock slopes. Rocscience Inc., Toronto
- Rocscience (2015d) RocTopple v.1-toppling analysis for rock slopes. Rocscience Inc., Toronto
- Rocscience (2015e) RocFall v. 5-statistical analysis of slopes at risk for rockfalls. Rocscience Inc., Toronto
- RocPro3D (2014) RocPro3D software. [https://www.rocpro3d.com/rocpro3d\\_en.php](https://www.rocpro3d.com/rocpro3d_en.php).
- Rouiller JD, Macro C (1997) Application de la méthodologie MATTEROCK á l'évaluation du danger lié aux falaises. *Eclogae Geologicae Helvetiae* 90:393–399
- Russell CP, Santi P, Humphrey JD (2008) Modification and statistical analysis of the Colorado rockfall hazard rating system: Report No. CDOT-2008-7, p 139
- San NE (2017) Investigation of rockfall around Ankara citadel, M.S. Thesis, 131 p.

- Saroglou H, Marinos V, Marinos P, Tsiambaos G (2012) Rockfall hazard and risk assessment: an example from a high promontory at the historical site of Monemvasia, Greece. *Nat Hazards Earth Syst Sci* 12:1823–1836
- Santi PM, Christopher PR, Jerry DH, Jessica IS (2009) Modification and statistical analysis of the Colorado rockfall hazard rating system. *Eng Geol* 104(1–2):55–65. <https://doi.org/10.1016/j.enggeo.2008.08.009>
- Schweigl J, Ferretti C, Nossing L (2003) Geotechnical characterization and rockfall simulation of a slope: a practical case study from south Tyrol (Italy). *Eng Geol* 67:281–296
- Scioldo G (1991) ISOMAP and ROTOMAP, 3D surface modelling and rockfall analysis. Geo and Soft, Torino
- Spang RM, Rautenstrauch RW (1988) Empirical and mathematical approaches to rockfall protection and their practical applications. In: *Proceeding of the 5th international symposium on landslides*. Rotterdam, Balkema, pp 1237–1243
- Stevens WD (1998) RocFall: a tool for probabilistic analysis, design of remedial measures and prediction of rockfalls. MSc. Thesis, University of Toronto
- Straub D, Schubert M (2008) Modelling and managing uncertainty in rock-fall hazards. *Georisk* 2(1):1–15
- TBC (2018) New Turkish Building Earthquake Code
- Teoman MB, Topal T, Işık NS (2004) Assessment of slope stability in Ankara clay: a case study along E90 highway. *Environ Geol* 45(7):963–977
- Tokmak M (2005) Documentation and examination of historic building materials for the purpose of conservation: case study, part of the walls at the Citadel of Ankara. MSc thesis. Middle East Technical University (unpublished).
- Topal T, Akin M, Ozden AU (2006) Analysis and evaluation of rockfall hazard around Afyon Castle, Turkey. In: *Proceedings of the 10th international congress IAEG 2006-Engineering geology for tomorrow's cities*, Nottingham, Paper No: 439.
- Topal T, Akin M, Ozden AU (2007) Assessment of rockfall hazard around Afyon Castle. *Environ Geol* 53(1):191–200
- Topal T, Akin MK, Akin M (2012) Rockfall hazard analysis for a castle in Kastamonu (Turkey). *Nat Hazards* 62(2):255–274
- TRB (2012) Rockfall-characterization and control. In Turner AK and Schuster RL, Transportation Research Board., Washington DC.
- TS 699 (2009) Methods of testing for natural building stones. Turkish Standards Institute (in Turkish).
- Tunusluoglu MC, Zorlu K (2009) Rockfall hazard assessment in a cultural and natural heritage (Ortahisar Castle, Capadocia, Turkey). *Environ Geol* 56(5):963–972
- Uribe-Etxebarria G, Morales T, Urarte JA, Ibarra V (2005) Rock cut stability assessment in mountainous regions. *Environ Geol* 48(8):1002–1013. <https://doi.org/10.1007/s00254-005-1323-1>
- Varnes DJ (1978) Slope Movement Types and Processes. In: Schuster RL, Krizek RJ (eds.) *Landslides: analysis and control*. Special Report 176, Transportation and Road Research Board, National Academy of Science, Washington, DC, pp. 11–33.
- Wang IT, Lee CY (2010) Influence of slope shape and surface roughness on the moving paths of a single rockfall. *World Acad Sci Eng Technol* 65:1021–1027
- Wasowski J, Gaudio VD (2000) Evaluating seismically induced mass movement hazard in Caramanico Terme (Italy). *Engi Geol* 58:291–311
- Wick E, Baumann V, Jaboyedoff M (2010) Report on the impact of the 27 February 2010 earthquake (Chile, Mw 8.8) on rockfalls in the Las Cuevas valley, Argentina. *Nat Hazards Earth Syst Sci* 10:1989–1993
- Wieczorek GF, Stock GM, Reichenbach P, Snyder JB, Borchers JW, Godt JW (2008) Investigation and hazard assessment of the 2003 and 2007 Staircase Falls rock falls, Yosemite National Park, California, USA. *Nat Hazards Earth Syst Sci* 8:421–432
- Woodard MJ, Shakoor A (2005) Development of a rockfall hazard rating matrix for Ohio. In: *Proceedings of international symposium on geology and linear infrastructures*. Lyon
- Wong CKL (1998) The new priority classification systems for slopes and retaining walls, GEO Report No.68. Geotechnical Engineering Office, Kowloon
- Wyllie DC (2015) *Rock fall engineering*. CRC Press, New York
- Wyllie DC, Mah CW (2004) *Rock slope engineering-civil and mining*, 4th edn. Spoon Press, London
- Youssef A, Maerz NH, Fritz MA (2003) A risk-consequence rockfall hazard rating system for Missouri highways. 54th Highway Geology Symposium, Burlington, Vermont, pp 175–195
- Zhu C, Wang D, Xia X, Tao Z, He M, Cao C (2018) The effects of gravel cushion particle size and thickness on the coefficient of restitution in rockfall impacts. *Nat Hazards Earth Syst Sci* 18:1811–1823

**Publisher's Note** Springer Nature remains neutral with regard to jurisdictional claims in published maps and institutional affiliations.